Exceptional Reduction of the Diffusion Constant in Partially Disordered Photonic Crystals

Costanza Toninelli,[1,*] Evangellos Vekris,[2] Geoffrey A. Ozin,[2] Sajeev John,[3] and Diederik S. Wiersma[1]

[1]*European Laboratory for Nonlinear Spectroscopy and INFM-BEC, Sesto Fiorentino (Florence), Italy*
[2]*Department of Chemistry, University of Toronto, Toronto, Ontario, Canada*
[3]*Department of Physics, University of Toronto, Toronto, Ontario, Canada*

(Received 7 February 2008; revised manuscript received 26 July 2008; published 15 September 2008)

In real photonic crystals light is scattered by the imperfections of the periodic potential. We study experimentally the propagation of diffused light in silicon inverse opals and report an exceptionally reduced diffusion constant of 3.0 ± 0.7 m^2/s, in samples which are only partially disordered. Waves scattered both by the lattice planes and by their imperfections interfere and light is efficiently trapped in this hybrid scattering regime. Not only higher quality crystals, but also random materials present an order of magnitude bigger diffusion constant and hence weaker scattering.

DOI: 10.1103/PhysRevLett.101.123901 PACS numbers: 42.25.Dd, 05.60.Cd, 42.70.Qs, 72.15.Rn

Transport of waves is an important concept in various fields, like solid-state and atomic physics, acoustics, and optics. Recent developments in the realization of photonic materials allow us to investigate light propagation in systems ranging from ordered photonic crystals [1] to quasicrystals [2] and controlled random materials [3]. In disordered systems, light undergoes multiple scattering which, to first order, can be described as a diffusion process. Interference, however, can lead to unexpected transport effects, of which maybe the most dramatic is that of Anderson localization. This phenomenon was originally predicted for electron transport [4] and later generalized to classical waves [5–7]. It produces an inhibition of transport and thus results in a vanishing diffusion constant, due to the formation of localized eigenstates.

Periodic optical materials, called photonic crystals, can also trap light. In these systems propagation is inhibited in certain frequency windows called photonic band gaps, due to destructive interference in the periodic structure [8]. In practice, a disorder-free periodic structure can hardly be realized so that usually both order and disorder play a role. The physics of (light) transport in such a partially ordered or disordered structure is potentially very interesting [9–11] but has yet to be fully explored. The more straightforward effect of imperfections is a reduction of the band gap efficiency, corresponding to the migration of new accessible states from the edge towards the band gap [12,13]. Much more intriguing is the prediction that strong localization of light can be facilitated by the reduction of the electromagnetic density of states in a photonic band gap material [14]. The subtle interplay between order and disorder is the basis of the work described in this Letter, where we present observation of extremely efficient trapping of light in a partially disordered photonic crystal.

We report on direct time-resolved measurements of diffuse light, close to the band gap of different silicon inverse opals [15] at increasing amounts of structural disorder. The static properties of the samples are independently characterized via reflection spectra and by means of absolute transmission measurements. Scanning-electron microscope (SEM) images are provided to further characterize the level of structural disorder. In certain lattices with significant partial disorder, we observe a huge reduction of the diffusion constant, which is even smaller than that of a fully random sample. We interpret the effect as being due to a renormalization of the diffusion constant by strong interference effects. This observation provides also the first step toward the demonstration of light localization in a 3D photonic band gap (PBG) material.

We have analyzed three materials of comparable thickness, all made in silicon, but with a different degree of structural order. In particular, the systems $M1$ and $M2$ are silicon inverse opals with very similar nominal parameters, grown under slightly different thermodynamic conditions. The fabrication process starts from a matrix of silica spheres assembled by dip-coating in an fcc lattice, then infiltrated with amorphous silicon ($n = 3.6$) by chemical vapor deposition [16]. In order to increase the stability of the template, a thin silica layer is deposited before the silicon infiltration. Chemical and reactive ion etching finally provides the removal of the silica opal. $M3$ is instead a completely random material, obtained by grinding a silicon wafer into a fine powder, where the average dimension of the grains is roughly comparable with the lattice constant of the photonic crystals ($a = 1188$ nm). As can be observed in the SEM pictures of Fig. 1, $M1$ and $M2$, despite having the same lattice constant and sphere polydispersivity, have a slightly different level of silicon infiltration and packing fraction of the spheres. In the Fourier transform of the image (insets), the diffraction peaks of material $M2$ appear blurred with respect to those of $M1$, clearly showing the presence of differently oriented domains within the dimension of the image [17]. For the third type of material, the presence of a single peak and the spherical symmetry in the Fourier transform are signatures of uncorrelated disorder. In the autocorrelation of the SEM images, plotted in the bottom panel of Fig. 1, $M1$ and $M2$ present oscillations on the same length scale, correspond-

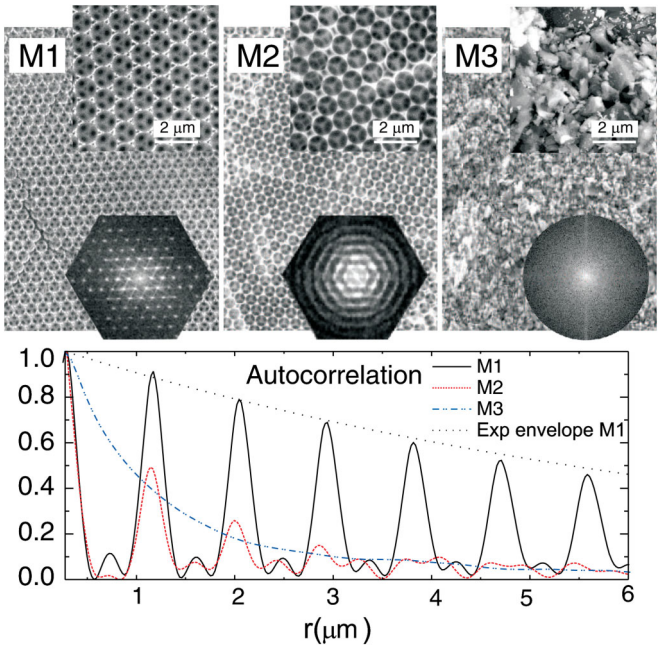

FIG. 1 (color online). Structural characterization of three different materials. The SEM images of the samples are shown, together with their Fourier transforms (inset) and linear autocorrelation function. The latter is calculated as the correlation between points at distance r along a line on the SEM image. The periodicity of the crystals yields an oscillating spatial correlation (solid and dotted curve), which is damped on different length scales, depending on the amount of imperfections. The dash-dotted curve corresponds to the autocorrelation of the random sample.

ing to the periodicity of the structure, but the decay of the envelope shows that $M1$ has more long range order. The exponential decay lengths are, respectively, 7.5 and 1.5 μm. The case of the random material where no oscillating features appear is different. Here the decay is a measure for the average grain size, which equals $\simeq 1$ μm.

The optical characterization of the samples comprises reflection measurements, performed with a tungsten lamp coupled to a spectrometer, equipped with a PbS infrared detector, working with a spectral resolution of 2 nm in the range from 800 to 2600 nm. The spot size on the sample surface is about 200 μm, thus introducing some spatial averaging. In Fig. 2 the reflection spectra are shown as collected at 10° of external incidence angle from the (1,1,1) plane of two silicon inverse opals of type $M1$-2, respectively, in panels (b) and (c), together with the band diagram (a) of the perfect crystal structure, calculated by plane wave expansion. In panel (d) the reflection spectrum of the random material is plotted for comparison.

The band structure was obtained by considering a model of interpenetrating air spheres (radius r) in an fcc geometry with cubic lattice constant a, coated with amorphous silicon shells of external radius R. We performed calculations varying the parameters R/a and r/a and found the best correspondence to our data with $r/a = 0.358$ and $R/a = 0.408$. This geometry corresponds to a realistic silicon

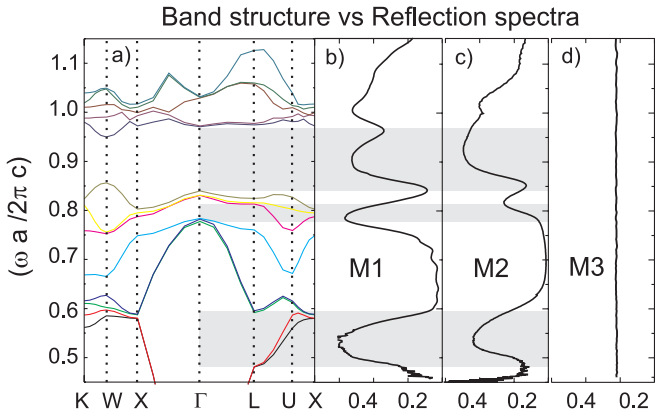

FIG. 2 (color online). Reflection measurements at normal incidence compared to the band diagram (a) of a highly ordered silicon inverse opal of type $M1$ (b), a more disordered one $M2$ (c), and the fine silicon powder representing material $M3$ (d). As for the periodic structures, one can recognize in the gray-highlighted regions different reflection peaks, at $\omega a/2\pi c = 0.55$ and 0.8, in correspondence with two pseudogaps in the $\Gamma - L$ direction and at $\omega a/2\pi c = 0.9$, relative to the predicted band gap.

filling fraction of the air voids of about 86% [18]. The first two experimental spectra both show the expected resonant features of inverse opals (gray-highlighted regions). Going from low to high energies, one can recognize the Bragg peak of the fundamental stop-gap in the ΓL direction, then a narrower structure corresponding to a higher stop-gap in the same direction, followed by the reflection peak, associated with the complete PBG. The latter has an average relative width $\Delta\omega/\omega$ limited at the W point to 5.5%, consistent with the values known in literature [19,20]. The extent of the reactive ion etching on the surface may determine the presence of strong surface resonances at high frequencies [21] and of a reflection plateau in the passband. As a consequence, the low level of reflection we observe in the passband for both photonic crystals can be interpreted as a signature of good surface polishing.

The two spectra in panels (b) and (c) differ substantially on at least three main points: (i) where the system is supposed to exhibit geometrical resonances, $M1$ presents higher reflectivity; (ii) $\Delta\omega/\omega$ for the first Bragg peak is larger for $M2$ ($\Delta\omega/\omega = 0.15$) than for $M1$ ($\Delta\omega/\omega = 0.14$); (iii) the whole spectrum of $M2$ is blue-shifted with respect to $M1$. Two factors can play a role in these differences, namely, the connectivity of the spheres constituting the opal matrix, and the level of silicon infiltration. From the observations (i) and (ii), materials of type $M2$ manifest the key signatures of more structural disorder, i.e., given the same photonic structure, a broader and lower reflection peak. The presence of disorder prevents us from directly associating a Bragg length to the peak width [11]. The third type of material $M3$ does not show any resonance in the spectrum and has by far the most structural disorder.

To further quantify with optical means the relative amount of disorder, we measured the scattering mean

free path ℓ_s by recording the absolute transmission at a given frequency in the pass band of the photonic crystals. Applying the Lambert-Beer law, our measurements yield ℓ_s equal to 5 μm for $M1$ and 2.8 μm for $M2$. The scattering mean free path of $M3$ depends on the dimension of the powder grains, the filling fraction, and the refractive index contrast, and is measured to be 3 μm.

In order to obtain information on light propagation in these materials, we have performed a time-resolved study to determine the light diffusion constant. Such dynamic measurements can provide crucial and, as in this case, even surprising information on how strong light is localized in a sample [22]. We recorded the multiply scattered light in transmission through the samples, in a time-resolved apparatus based on optical gating (described, e.g., in Ref. [23]), using short (150 fs pulse duration) laser pulses, with a wavelength tunable between 1400 and 1600 nm. The setup is aligned such that no residual direct transmission and only multiply scattered light is collected. The diffusely transmitted light is mixed in a nonlinear beta-barium borate crystal with a reference pulse travelling on a delay line. The generated nonlinear signal is proportional to the cross correlation between the probe and the reference pulse. An example of such an observed temporal response of the samples is reported in Fig. 3, for different degrees of structural order. The typical diffuse transmission through a disordered sample is characterized by an exponentially decaying curve at long times, which depends on the sample thickness and diffusion coefficient. We can observe that a photonic crystal of type $M2$ with more structural disorder than $M1$ exhibits an extremely slowly decaying signal, which corresponds to a very small value of the diffusion constant, hence to strong scattering. Note that the thickness of the samples is comparable. [For the measurements in Fig. 3 we have $L(M1) = 17 \pm 2$ μm; $L(M2) = 12.5 \pm 1.5$ μm; $L(M3) = 20 \pm 3.5$ μm]. Naively one would now expect that by further increasing the structural disorder, the scattering would even increase. The random material $M3$, with comparable thickness, refractive index

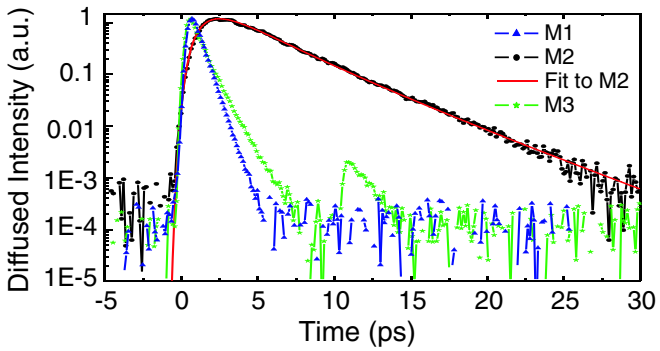

FIG. 3 (color online). Diffusive propagation of light at $\lambda = 1500$ nm ($a/\lambda = 0.8$) through three silicon materials. The partially ordered sample (small circles) clearly exhibits the slowest diffusion. The solid curve is a fit with a solution to the diffusion equation.

contrast, and analogous filling fraction, on the other hand, exhibits a much faster decay [24]. The partially disordered photonic crystal is clearly the strongest scattering system, by nearly an order of magnitude. The decay time of the diffuse signal, which represents the residence time of the diffuse light in the sample, is $\tau \simeq 490$ fs, $\tau \simeq 2.9$ ps, and $\tau \simeq 760$ fs, for $M1$-2-3, respectively. This surprising result shows that the interplay between order and disorder can strongly increase the scattering and trap the light more efficiently than a completely disordered structure.

In order to quantify these diffusive transport measurements, we fitted our data with a function (solid curve in Fig. 3) obtained as the convolution between a Gaussian pulse, whose width is given by the experimental one, and a solution to the diffusion equation [25]. The resulting effective diffusion coefficients are extraordinary. In particular the diffusion constant corresponding to $M2$ is equal to 3.0 ± 0.7 m^2/s. The error is mainly due to the uncertainty in the sample thicknesses, measured independently under a microscope at different points. Both a lower ($M1$) or a higher ($M3$) degree of structural disorder correspond to larger diffusion constants of 40 ± 10 m^2/s and 50 ± 17 m^2/s, respectively. The results are reproducible, in the sense that several samples, given the level of structural disorder, show similar diffusion constants. The effect of absorption is considered in the fits, resulting in an inelastic time of 20 ± 5 ps, consistent with the values quoted in literature for comparable amorphous silicon structures [26,27]. Note that an increased absorption will accelerate the decay in transmission and not slow it down; hence, the extremely slow diffusion in $M2$ cannot be due to absorption artifacts. We conclude that, in this regime, relevant interference effects, influencing either the mean free path or the transport velocity, yield a substantial renormalization of the Boltzmann diffusion constant.

It is instructive to associate a length scale ℓ to the diffusion process, assuming a relation of the form $D = 1/3v\ell$. In a random material one would interpret this ℓ as a transport mean free path and v would be the transport velocity v_e [28]. No theory is currently available for the transport velocity in disordered photonic crystals. However, to first approximation we can use for v the group velocity averaged over the Fermi surface [29]. For a sample of type $M2$, in the frequency window of the measurements, this gives 3.0×10^7 m/s, leading to an estimated value for ℓ as small as 300 ± 100 nm. Estimating the velocity v in the medium using a geometrically averaged effective refractive index yields an even smaller ℓ.

In Fig. 4 we have plotted the dependence of the measured diffusion constant on wavelength, together with the measured reflection spectrum and calculated density of states (DOS) of the ideal photonic structure. (The latter therefore does not take into account any changes in the DOS induced by the disorder.) Over the wavelength range of approximately 200 nm that was accessible in our experiments we did not observe any variation in the value of the diffusion constant larger than about 25%. Note that this

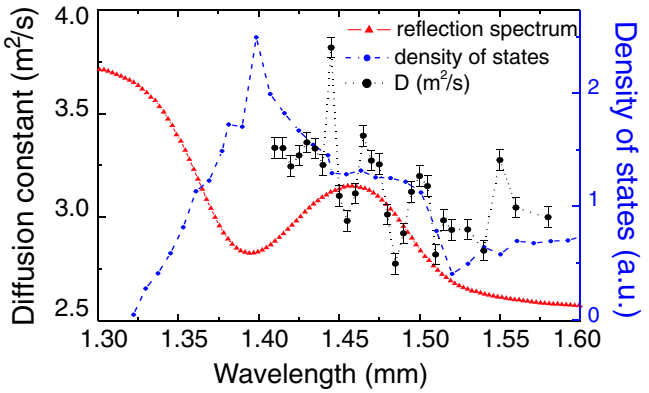

FIG. 4 (color online). Diffusion constant for inverse opal ($M2$) as a function of wavelength. On the same x axes are plotted (triangles) the reflection spectra, collected on the same point and under the same incident angle and (small circles) the calculated density of states of the electromagnetic field in the photonic crystal.

extremely small value of the diffusion constant is measured in the band edge region of the perfect photonic crystal and not in the band gap. There does not seem to be a straightforward relation between the density of states of the underlying perfect structure and the diffusion constant, although there is a trend that the diffusion constant decreases upon decreasing DOS. The picture is complicated because scattering creates new accessible states (and hence modifies the DOS) and interference effects act both on the effective mean free path and transport velocity.

In conclusion, we have observed a strong reduction of the diffusion coefficient in a disordered photonic crystal. The smallest value of the diffusion constant is found in a material with partial order/disorder, hence indicating that it is the combined effect of order and disorder that leads to such a large renormalization of the Boltzman diffusion constant. A complete theory that can deal with multiple scattering in a system with long-range order would be required to understand better the relation between the density of states and the diffusion constant. The surprising observation that a material with partial order can give rise to stronger scattering compared to a completely disordered structure shows how rich the physics is of light transport in photonic materials.

We wish to thank S. Gottardo and F. Riboli for stimulating discussions and N. Tétreault for his help in sample preparation. We acknowledge financial support from the EC NoE Phoremost, EU Contract No. RII3-CT-2003-506350, and the Natural Sciences and Engineering Research Council of Canada.

*toninelli@lens.unifi.it; www.complexphotonics.org

[1] K. Busch *et al.*, Phys. Rep. **444**, 101 (2007).
[2] W. Man, M. Megens, P. J. Steinhardt, and P. M. Chaikin, Nature (London) **436**, 993 (2005); A. Ledermann *et al.*, Nature Mater. **5**, 942 (2006).
[3] P. D. Garcìa, R. Sapienza, À. Blanco, and C. López, Adv. Mater. **19**, 2597 (2007).
[4] P. W. Anderson, Phys. Rev. **109**, 1492 (1958).
[5] S. John Phys. Rev. Lett. **53**, 2169 (1984).
[6] P. W. Anderson, Philos. Mag. B **52**, 505 (1985).
[7] A. Lagendijk, M. P. van Albada, and M. B. van der Mark, Physica A (Amsterdam) **140**, 183 (1986).
[8] *Photonic Bandgap Materials*, edited by C. M. Soukoulis (Kluwer, Dordrecht, 1996); J. D. Joannopoulos, R. D. Meade, and J. N. Winn, *Photonic Crystals: Moulding the Flow of Light* (Princeton University Press, Princeton, NJ, 1995).
[9] S. John, Phys. Rev. Lett. **58**, 2486 (1987).
[10] A. F. Koenderink and W. L. Vos, Phys. Rev. Lett. **91**, 213902 (2003); A. F. Koenderink *et al.*, Phys. Lett. A **268**, 104 (2000); V. Yannopapas, A. Modinos, and N. Stefanou, Phys. Rev. B **68**, 193205 (2003); T. Schwartz *et al.*, Nature (London) **446**, 52 (2007); J. Topolancik, B. Ilic, and F. Vollmer, Phys. Rev. Lett. **99**, 253901 (2007).
[11] J. Huang *et al.*, Phys. Rev. Lett. **86**, 4815 (2001).
[12] M. A. Kaliteevski, D. M. Beggs, S. Brand, R. A. Abram, and V. V. Nikolaev, Phys. Rev. B **73**, 033106 (2006).
[13] Y. A. Vlasov, M. A. Kaliteevski, and V. V. Nikolaev, Phys. Rev. B **60**, 1555 (1999).
[14] S. John and R. Rangarajan, Phys. Rev. B **38**, 10101 (1988).
[15] A. Blanco *et al.*, Nature (London) **405**, 437 (2000).
[16] N. Tétreault *et al.*, Adv. Mater. **15**, 1167 (2003).
[17] E. Vekris *et al.*, Adv. Mater. **20**, 1110 (2008).
[18] D. Gaillot, T. Yamashita, and C. J. Summers, Phys. Rev. B **72**, 205109 (2005).
[19] K. Busch and S. John, Phys. Rev. E **58**, 3896 (1998).
[20] A. F. Koenderink, A. Lagendijk, and W. L. Vos, Phys. Rev. B **72**, 153102 (2005).
[21] F. Garcia-Santamaria, E. C. Nelson, and P. V. Braun, Phys. Rev. B **76**, 075132 (2007).
[22] A. A. Chabanov, Z. Q. Zhang, and A. Z. Genack, Phys. Rev. Lett. **90**, 203903 (2003); S. E. Skipetrov and B. A. van Tiggelen, Phys. Rev. Lett. **96**, 043902 (2006); M. Störzer, P. Gross, C. M. Aegerter, and G. Maret, Phys. Rev. Lett. **96**, 063904 (2006).
[23] R. Sapienza *et al.*, Phys. Rev. Lett. **91**, 263902 (2003).
[24] The second lower peak in the diffusion profile from $M3$ is due to an internal front-end reflection from the glass substrate.
[25] D. S. Wiersma, A. Muzzi, M. Colocci, and R. Righini, Phys. Rev. E **62**, 6681 (2000).
[26] G. Moddel, D. A. Anderson, and W. Paul, Phys. Rev. B **22**, 1918 (1980).
[27] M. Dinu *et al.*, Appl. Phys. Lett. **82**, 2954 (2003).
[28] M. P. van Albada, B. A. van Tiggelen, A. Lagendijk, and A. Tip, Phys. Rev. Lett. **66**, 3132 (1991).
[29] Note that the Mie resonances that are important for v_e in random collections of monodisperse spheres [28] do not play a role in our samples, since inverse structures have nearly no resonant behavior and scattering is determined by small, irregular imperfections instead of spheres.